

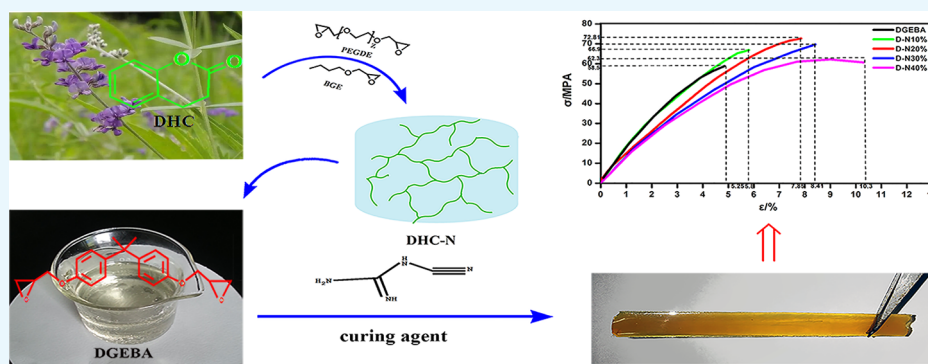
Renewable Coumarin-Derived Network as a Toughening Structure for Petroleum-Based Epoxy Resins

Xiaoxia Cai,[†] Cong Li,^{*,‡} Congde Qiao,[†] and Dan Peng[§]

[†]Key Laboratory of Processing and Testing Technology of Glass Functional Ceramics of Shandong Province, School of Materials Science and Engineering, Qilu University of Technology and [‡]State Key Laboratory of Biobased Material and Green Papermaking, Qilu University of Technology, Shandong Academy of Sciences, Jinan 250353, P. R. China

[§]Advanced Materials Institute, Qilu University of Technology, Shandong Academy of Sciences, Jinan 250014, P. R. China

Supporting Information



ABSTRACT: A double-network strategy to toughen epoxy resin system is presented herein. Dihydrocoumarin (DHC), a hexatomic compound extracted from tonka bean, is used as the building block for the construction of the first network, and the diglycidyl ether of bisphenol A epoxy matrix is used as the second network. The resultant double network demonstrates a single glass transition and good compatibility between these two networks. Owing to the firm interfacial adhesion between networks and the effective stress transfer as well as external energy absorption derived from the DHC-based network, the double-network-based epoxy resin shows a significant toughness improvement without trade-offs in the tensile strength and elongation at break. The finding in this study provides a promising way to overcome the intrinsic brittleness of commercial epoxy resin via the utilization of renewable DHC for the construction of a novel double network.

INTRODUCTION

Epoxy resins are widely used in electrical insulators, composites, coatings, and adhesives due to their superior mechanical strength and chemical resistance.^{1–3} However, the inherent brittleness and poor impact resistance due to its highly cross-linked network structure limits the application of epoxy resin as a load-bearing material, especially in some harsh environments like automotive and aerospace fields.⁴

Overcoming the intrinsic brittleness is significant for epoxy resins, and extensive efforts have been devoted to improving the resin toughness over the last decades.^{5–8} These works are generally performed via the incorporation of thermoplastic or inorganic fillers like rubber-based core–shell particles, silica, and nanoparticles into the resin matrix.^{9–14} These fillers act as the dispersed phase to absorb energy and terminate the crack propagation by bonding with the resin matrix, thereby toughening and reinforcing the epoxy.^{5–17}

In recent years, green approaches derived from natural resources have emerged to toughen the epoxy resin, as they are available, environmentally friendly, non-noxious, and renewable.^{18–20} Among these approaches, using plant oil or their

derivates as a modifier is an important strategy to toughen the epoxy resin system.^{21–23} Utilizing blending and copolymerization of these plant oil derivates in the epoxy mixture, effective improvement in impact strength can be achieved. However, it is noteworthy that an obvious decrease in tensile strength occurs with the introduction of these plant oil derivates into the epoxy system.²⁴ This is due to the lack of interfacial interaction between the epoxy matrix and the plant oil additives. Fei et al. chemically modified the surface of tannic acid (TA) through the ring-opening reaction between TA and 1,2-epoxydodecane in the presence of triphenylphosphine catalyst.²⁵ This modified TA has good dispersion in the diglycidyl ether of bisphenol A (DGEBA) matrix and can be used as an effective toughening agent without the trade-off of tensile strength. Using branched polymers to toughen the epoxy resin is another effective strategy due to their spherical arrangement and the adhesion with the matrix via the surface

Received: July 23, 2019

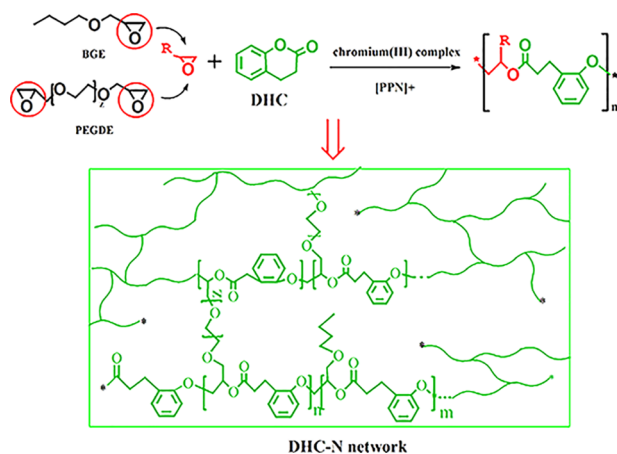
Accepted: September 5, 2019

Published: September 18, 2019

functional groups. Wang et al. had synthesized a branched triscardanyl phosphate (PTCP), comprising phosphaphenanthrene groups, from biobased cardanol. Compared to the neat DGEBA, the addition of 20 wt % PTCP leads to an improvement in impact strength, tensile strength, and elongation at break simultaneously.²⁶ This toughening effect is attributed not only to the rigid benzyl groups but also the hydroxyl groups attached on the branched chains. These hydroxyl groups could react with the DGEBA epoxy groups to enhance the interfacial adhesion. Clearly, the toughening effect is highly correlated to the interfacial adhesion of the epoxy matrix and the toughening agent. Firm interfacial adhesion plays an important role in effectively transferring external stress from the epoxy matrix to the toughening agent phase. In this way, the brittle epoxy resin would have a better performance in the impact resistance compared to those with poor interfacial adhesion.

In addition to the approaches mentioned above, double-network strategy is another emerging approach showing promising perspective in the toughening of polymeric materials.²⁷ Compared to the modification of the surface of the toughening agents to improve the interfacial adhesion, the double network can achieve this effect via the forced compatibility between the epoxy phase and the toughening agent phase.²⁸ Reasonable network design within the polymeric matrix is the key factor for the successful construction of the double network. Dihydrocoumarin (DHC, chemical structure is shown in Scheme 1) is an

Scheme 1. Ring-Opening Reaction of Poly(ethylene glycol) Diglycidyl Ether (PEGDE), Butyl Glycidyl Ether (BGE) with DHC and the Formation of DHC-N Networks



appealing monomer that is derived from coumarin, a renewable feedstock from tonka bean with a hexatomic ring structure. Due to the modest ring strain, DHC can achieve alternative copolymerization with an epoxy group via the ring-opening reaction to obtain polyesters with high molecular weight.^{29,30} In this research, we intend to fabricate a DHC-based network (i.e., DHC-N) via solvent-free chromium(III) salen-mediated pathway and use it as the first network. Diglycidyl ether of bisphenol A (DGEBA), the most widely used commercial epoxy resin, is used as the second network. A double network can be constructed via introducing the DHC-based network (DHC-N) into the relatively rigid DGEBA matrix. In addition to the forced compatible effect via the double-network strategy, similar phenyl moiety existing both in

DGEBA and DHC is also beneficial to their compatibility. It is expected that this novel DHC-based network plays a vital role in stress transfer and external energy absorption, whereby DGEBA epoxy system can achieve remarkable performance improvement in terms of impact strength, tensile strength, and elongation at break simultaneously.

RESULTS AND DISCUSSION

DHC-N Network. The modest ring strain in DHC monomer provides the possibility of achieving an alternative copolymerization with epoxides via the metal-mediated catalysis approach.³⁰ Here, chromium(III) complex was used as the Lewis acid to activate the ring-opening of epoxide and [PPN]⁺ serves as counterion to form a chromium(III) alkoxide. To construct a cross-linked network rather than a linear structure, the poly(ethylene glycol) diglycidyl ether (PEGDE) with two terminal epoxy groups was applied here as one of the building blocks. Scheme 1 displays the synthesis of the DHC-N network using the alternating copolymerization of DHC, PEGDE, and BGE.

The chain propagation and molecular weight growth in the initial synthesis stage of the DHC-N network were measured by GPC (Figure 1 and Table 1). Table 1 displays the increase

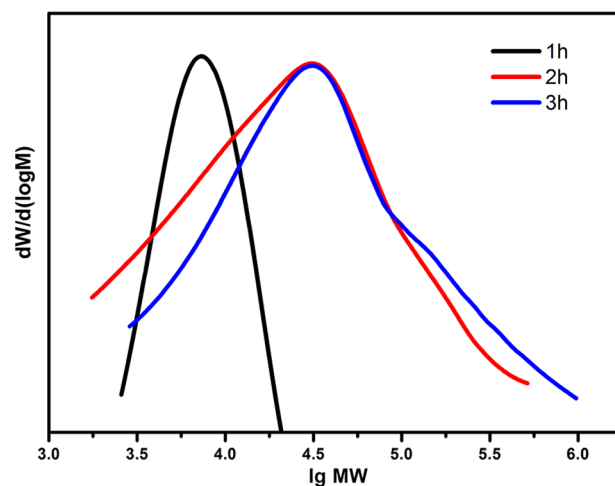


Figure 1. GPC chromatograms reflecting the molecular weight variation of the DHC-N network in the initial synthesis stage at 1, 2, and 3 h, respectively.

Table 1. Molecular Weights and Distributions of DHC-N Network with the Reaction Time at 80 °C

samples	M_n (Da)	M_w (Da)	M_p (Da)	M_z (Da)	polydispersity
DHC-N 1 h	5942	8988	4457	15 760	1.512
DHC-N 2 h	9865	41 760	10 410	193 600	4.233
DHC-N 3 h	13 690	71 740	12 240	316 900	5.241

of the average molecular weight (e.g., M_n , M_w , M_p , M_z) with the reaction time at 80 °C. Clearly, the growth of the molecular weight is attributed to the alternative ring-opening reaction of the epoxy ring and the DHC ring with the aid of a catalyst. Compared to the M_p at reaction time of 1 h, the counterpart undergoing a 2 or 3 h reaction has a much higher value, implying a significant molecular weight increase within 2 h. Besides, the higher polydispersity after 2 or 3 h reaction indicates that in addition to the higher molecular weight fraction, the relatively lower ones still exist. The chemical

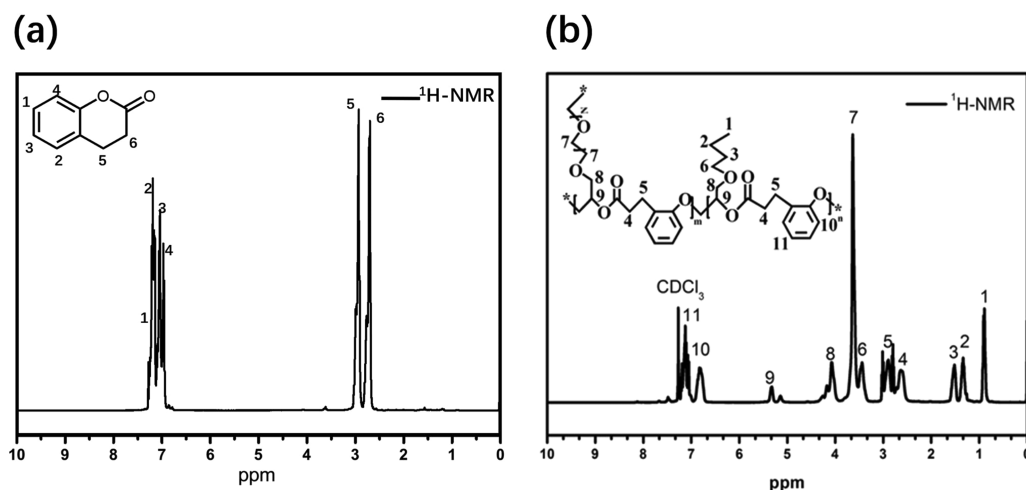


Figure 2. ^1H NMR spectra of DHC (a) and DHC-N network (b).

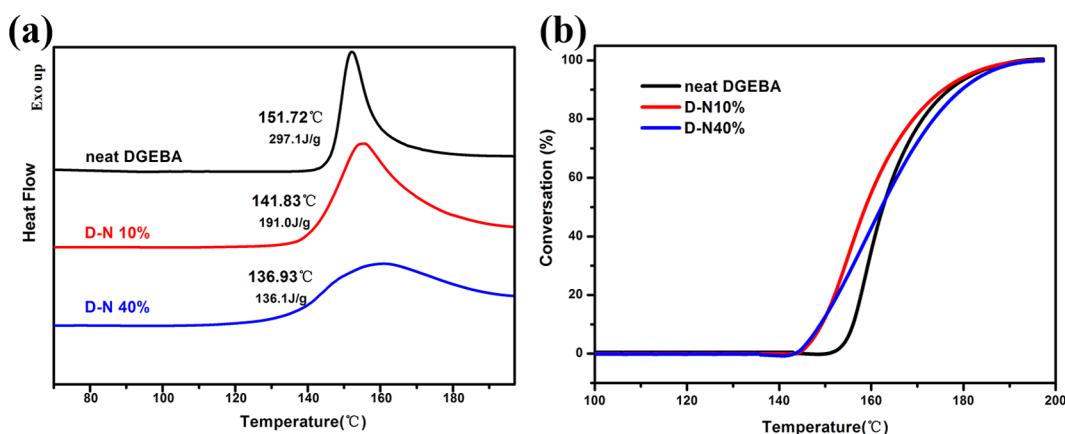


Figure 3. (a) DSC thermograms of neat DGEBA, D-N 10%, and D-N 40%. (b) Conversion degree against temperature during the curing process of neat DGEBA, D-N 10%, and D-N 40%.

structure features of DHC and DHC-N were represented via NMR spectra (Figure 2). The signals in the range of 7.25–6.70 ppm are attributed to the aromatic moieties of the DHC. The signal at 3.63 ppm corresponds to the methoxy group ($-\text{CH}_2-\text{O}-$) derived from the PEGDE segment. The signals in the range of 2.52–3.00 ppm are associated with the protons of methylene in the DHC segment. The signals at 0.75, 1.14, and 1.29 ppm belong to the methyl and methylene moieties of the BGE segment, respectively.

DGEBA-Based Double Network (D-N). The double network (D-N) can be constructed via the immersion of the DHC-N into the DGEBA monomers and the subsequent polymerization with the aid of DICY (Figure S1). The curing behaviors of D-N and the neat DGEBA are described via the differential scanning calorimetry (DSC) exothermic curves (Figure 3). Compared to the neat DGEBA, the exothermic peak temperature of D-N does not change too much (Figure 3a). On the other hand, an obvious decrease in the starting conversion temperature can be observed in the conversion against temperature curve (Figure 3b). With increase in DHC-N loading, the starting conversion temperature shifts to a lower value. This that means the DHC-N existing in the double network has a positive effect on lowering the curing temperature of DGEBA.

Figure 4 shows the Fourier-transform infrared (FTIR) spectra of neat DGEBA, DHC, DHC-N, and cured D-N. It can

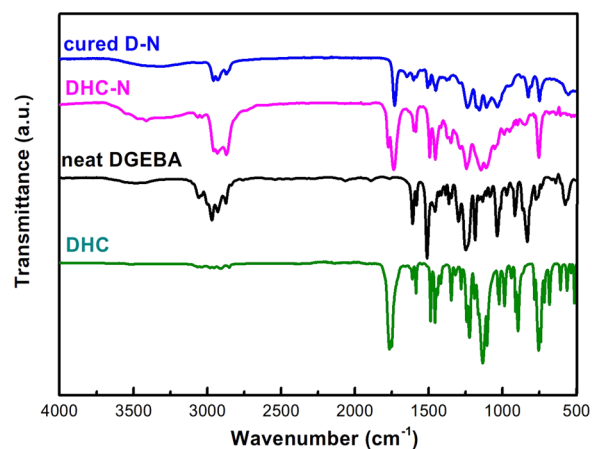


Figure 4. FT-IR spectra of neat DGEBA, DHC, DHC-N, and cured D-N.

be seen from the figure that these four curves are similar with the following absorption peaks: the peaks at 3000–2800 cm^{-1} are the characteristic signals of C–H stretching vibration and the peaks at 1530–1470 cm^{-1} are the characteristic signals of aromatic moiety. Compared to the neat DGEBA, the strong absorption peaks at 1750–1720 and 1200–1100 cm^{-1} are attributed to the carbonyl ($\text{C}=\text{O}$) group and ether ($\text{C}-\text{O}-\text{C}$)

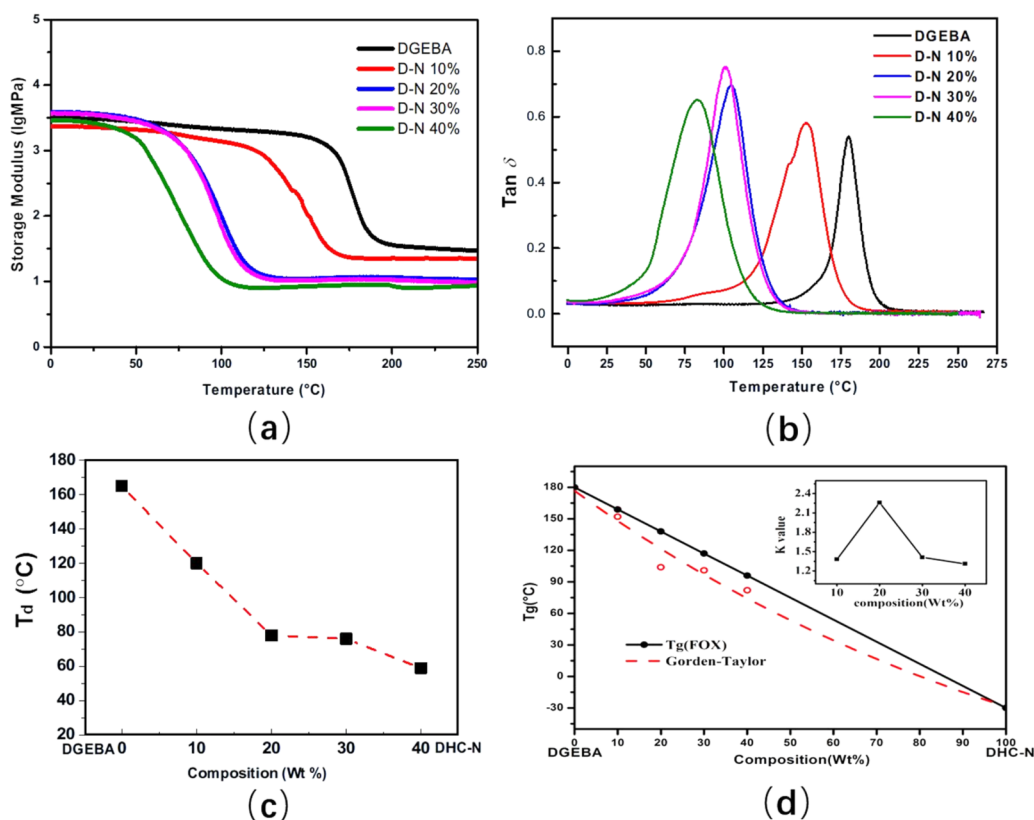


Figure 5. Storage modulus (a) and $\tan \delta$ (b) versus temperature for the neat DGEBA and the D-N-modified epoxy resins with different DHC-N loadings. (c) Onset temperature, T_d (i.e., a temperature at which storage modulus starts to decline significantly), of the D-N modified epoxy resin as a function of the DHC-N loading. (d) T_g composition behavior of the blends: (O) T_g measured from DMA and (●) T_g calculated based on Fox equation, and the k values shown in the inset are calculated based on the Gorden-Taylor equation.

group, respectively, that exist in DHC, DHC-N, and cured D-N networks. Moreover, it is noteworthy that, as the D-N FTIR curve shows, the characteristic epoxy peak ($850\text{--}800\text{ cm}^{-1}$) of neat DGEBA disappeared after undergoing a curing process with the DHC-N network. This indicates that the epoxy rings in DGEBA monomers were consumed via the ring opening of epoxy groups in the D-N construction process.

Thermal and Mechanical Properties. The dynamic mechanical properties of neat DGEBA and the DHC-N incorporated epoxy resins have been investigated by the dynamic mechanical analysis (DMA). As Figure 5a shows, the DHC-N loading influences the storage modulus significantly. Compared to the neat DGEBA, the temperature (T_d) at which the storage modulus started to decline shifted to a lower value of $125\text{ }^\circ\text{C}$ after 10 wt % DHC-N was introduced into the DGEBA matrix. This can be attributed to the flexible polyether structures contained in the DHC-N network. The polyether structures derived from the PEGDE and BGE monomers have a lower internal barrier, which leads to an easy chain rotation and significant lowering of the temperature at which the storage modulus starts to decline. As Figure 5c shows, the onset temperature T_d keeps decreasing with increase of DHC-N loading; however, it is noteworthy that this decreasing tendency begins to slow down when the DHC-N loading is higher than 20 wt %. This probably indicates that a fully developed DHC-N network was built within the epoxy resin when its content was higher than 20 wt %, so that the storage modulus is relatively stable and less susceptible to variation of the DHC-N content.

The compatibilities of the DGEBA matrix network and the DHC-N network are investigated via the dynamic mechanical analysis. The single loss peak during the entire temperature range indicates a good compatibility between the DGEBA matrix and the DHC-N portion (Figure 5b). For binary compatible blends, the glass transition can be predicted via the Fox equation or Gorden-Taylor equation.³¹ The Fox equation can be expressed as follows

$$T_g = w_1 T_{g1} + w_2 T_{g2} \quad (1)$$

The Gorden-Taylor equation can be expressed as follows

$$T_g = (w_1 T_{g1} + k w_2 T_{g2}) / (w_1 + k w_2) \quad (2)$$

where T_g is the glass transition of the blend and w_i is the weight fraction of component i . The interaction of these two components can be reflected by the k value. A k value higher than 1 suggests a stronger interaction of the two components in comparison with the self-interaction of the single component; in contrast, a k value lower than 1 suggests a relatively weaker interaction compared to the self-interaction. For the binary system studied here, the k values are higher than 1 in the entire DHC-N loading range (Figure 5d), indicating that the interaction between the DGEBA matrix and the DHC-N network is stronger compared to the self-interaction of the single network itself. This result is attributed to the specific double network and the correlated chemical structures. It is noteworthy that both DGEBA and DHC have the phenyl moiety. The similar phenyl moiety is beneficial to the interaction and compatibility of the DGEBA epoxy/DHC-N

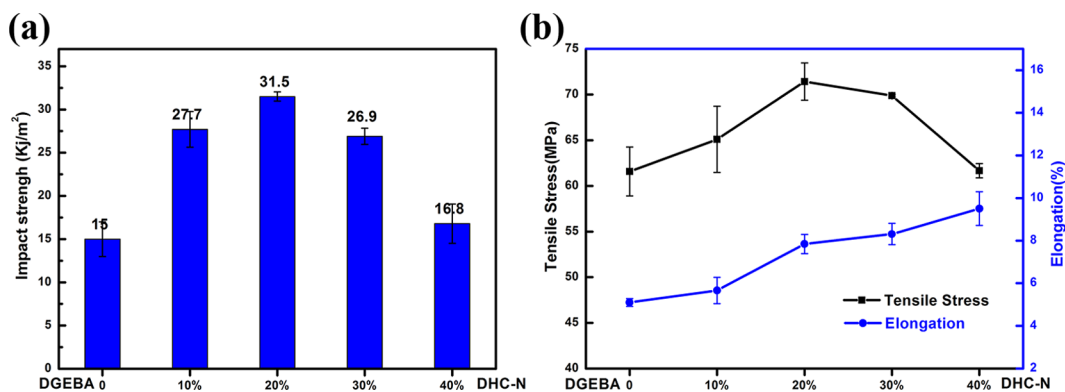


Figure 6. Impact (a) and tensile (b) properties of DGEBA and D-N-modified epoxy resins.

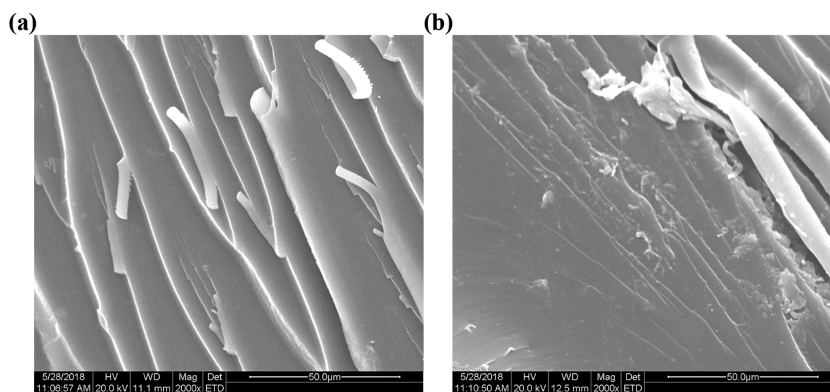


Figure 7. SEM images of fracture surface morphology: (a) neat DGEBA epoxy and (b) D-N-modified epoxy resin with 20 wt % DHC-N loading.

bionetwork. Moreover, the double-network structure plays an important role in the forced compatibility and the enhanced interaction in this binary system.

Toughening effect of the double network on the epoxy resin is investigated by the impact and tensile tests. The results are displayed in Figure 6. Remarkable improvement in impact strength was achieved after the incorporation of the DHC-N bionetwork. Thermoset with a 20 wt % DHC-N loading shows the best toughening effect and the highest impact strength of 31.5 kJ/m², which is almost twice the value of the neat epoxy (15 kJ/m²). More importantly, the increase in impact strength is achieved without impairing the tensile strength, which is verified by the tensile test. As Figure 6b shows, a continuous increase in tensile strength can be observed with the increase of the DHC-N loading, and the highest impact strength and tensile strength are obtained simultaneously when the DHC-N loading reaches up to 20 wt %. As discussed in the DMA storage modulus analysis, the decreasing tendency of T_d slows down when the DHC-N loading reaches 20 wt %. This value is consistent with that observed in the mechanical strength test, in which the highest impact strength and tensile strength are achieved at a DHC-N loading of 20 wt %. Therefore, it is speculated that 20 wt % is the threshold for the construction of the double network. Below this threshold, the DHC-N network is not fully developed within the epoxy resin and the mechanical properties (e.g., impact strength, tensile strength) continue to increase with increase of the DHC-N loading; above this threshold, excess DHC-N components lead to a more flexible network and reduce the overall mechanical strength. For the double network studied here, experimental data show that 20 wt % DHC-N is the optimal loading to

achieve the best mechanical performance (e.g., the highest impact strength and tensile strength). At this loading level, the external stress and impact experienced by the DGEBA epoxy would be effectively transferred and absorbed via the relatively flexible DHC-N bionetwork to retard the rupture of the entire network.

The toughening effect and fracture behavior of the epoxy resins were further revealed by the SEM micrographs (Figure 7). Sharp and smooth morphology can be clearly recognized for the neat DGEBA (Figure 7a), indicating a typical brittle fracture and a relatively low impact strength. When 20 wt % loading of DHC-N was added into the epoxy, a rougher fracture surface with more fibrils was formed (Figure 7b), indicating the specimen was broken in a more yielding way. The fibrils observed on the fracture surface are attributed to the fast crack growth, shear yielding, and coalescence of these microcracks,^{32,33} whereby excessive energy could be absorbed to improve the toughness of the epoxy resin. As Figure 7b shows, no phase separation was observed on the fracture surface when 20 wt % DHC-N was incorporated into the epoxy resin. This image reveals a good compatibility of the DHC-N portion and the DGEBA matrix, which is consistent with the signal loss peak observed in the DMA measurement.

Figure 8 shows the thermogravimetric behaviors of the neat DGEBA epoxy and the D-N-modified resins with different DHC-N loadings. Compared to the neat epoxy DGEBA, the DHC-N displays a significantly lower thermal degradation temperature at around 250 °C. However, once DHC-N is incorporated into the DGEBA to form a double network, the typical thermal degradation temperature of around 250 °C disappeared and a higher degradation temperature of around

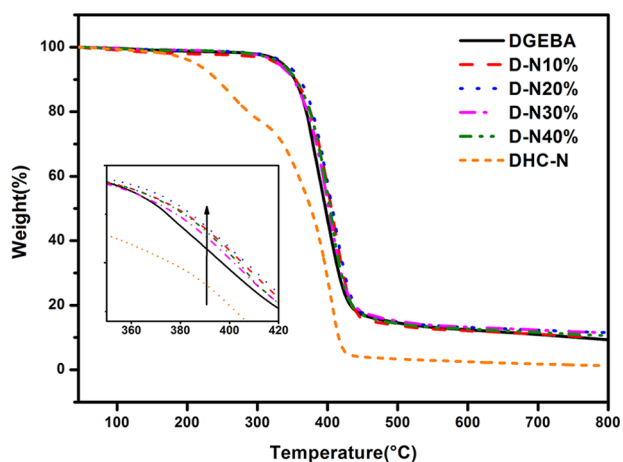


Figure 8. TGA curve of DGEBA, DHC-N, and D-N-modified epoxy resins with different DHC-N loadings.

400 °C was observed. This fact can be attributed to the good compatibility of the DHC-N bionetwork and the DGEBA epoxy resin via the forced compatible effect derived from the double network, which, in turn, produces a greater adhesion between the DHC-N network and the epoxy DGEBA matrix to prevent the elimination of the volatile fragments. Furthermore, the incorporation of the DHC-N network into the DGEBA matrix also slightly enhances the thermal stability of the entire system as shown by the increased degradation temperatures in the inset.

CONCLUSIONS

This paper reports a new method of toughening epoxy resin via fabricating a DHC-based network through a solvent-free chromium(III) salen-mediated pathway. This DHC-based network (DHC-N) is derived from renewable coumarin, and the single loss peak observed in the DMA measurement proved that this newly developed network is well-compatible with the epoxy resin system. A double-network structure can be constructed via the introduction of the DHC-based network into the DGEBA matrix. Prominent improvement in the mechanical performance was achieved through the double-network strategy; with 20 wt % DHC-N loading, the thermoset epoxy showed the highest impact strength of 31.5 kJ/m², which is almost twice the value of the neat epoxy (15.0 kJ/m²). Besides, the tensile strength and elongation at break were also increased by 14 and 45% respectively, reaching values of 71 MPa and 8%, respectively. The interaction between the DGEBA matrix network and the DHC-based network was described via the Gordon-Taylor equation and the *k* values higher than 1 indicated that stronger interactions existed between these two networks in comparison with the self-interactions existing in the single network itself. SEM was further conducted to investigate the feature of the fracture surface of the specimen. Compared to the neat DGEBA epoxy resin, the double-network-based epoxy resin demonstrated a rougher fracture surface with more fibrils, indicating that the DHC-N network plays a vital role in stress transfer and external energy absorption, whereby a significant improvement in epoxy toughness was obtained without a trade-off of its tensile strength and elongation at break.

EXPERIMENTAL SECTION

Materials. Diglycidyl ether of bisphenol A (DGEBA, EEW: 227 g/equiv), dihydrocoumarin (DHC, ≥98%), butyl glycidyl ether (BGE, 99%), poly(ethyleneglycol) diglycidyl ether (PEGDE, average *M_n* 500), (*S,S*)-*N,N'*-bis(3,5-di-*tert*-butylsilylidene)-1,2-cyclohexanediaminochromium(III) chloride, bis(triphenylphosphoranylidene)ammonium chloride, and dicyandiamide (DICY) were all purchased from Sigma-Aldrich.

DHC-Based Network (DHC-N) Preparation. The first network DHC-N was synthesized via the reaction of dihydrocoumarin (DHC), butyl glycidyl ether (BGE), and poly(ethylene glycol) diglycidyl ether (PEGDE) with the aid of catalysts (*S,S*)-*N,N'*-bis(3,5-di-*tert*-butylsilylidene)-1,2-cyclohexanediamino-chromium(III) chloride and bis(triphenylphosphoranylidene) ammonium chloride in a molar ratio of 1.1:0.6:0.2:0.04:0.04. The mixture comprising the reagents mentioned above was charged into a flask and stirred at 80 °C for 3 h and 120 °C for 0.5 h to obtain a sticky matter named as DHC-N.

Double Network (D-N) Preparation. DHC-N was then impregnated in the DGEBA matrix containing 5 wt % curing agent dicyandiamide (DICY) and 3 wt % accelerator in weight ratios (DHC-N/DGEBA) of 1:9, 2:8, 3:7, and 4:6, respectively. Resultant products were designated as D-N 10%, D-N 20%, D-N 30%, and D-N 40%, respectively. As a comparison, the single-network structure formed by the curing of the neat DGEBA was used as the second network.

Preparation of the Curing Mixtures. The D-N mixture was stirred at 80 °C for 30 min and then transferred to a poly(tetrafluoroethylene) mold for further curing. A fully cured resin was obtained after undergoing a curing process at 100 °C for 2 h and 150 °C for 5 h.

Characterizations. Gel permeation chromatography (GPC) was used to measure the molecular weight and molar mass distribution of the DHC-N at different reaction times. *N,N*-Dimethyl formamide (DMF) was used as the eluent at a flow rate of 1 mL/min.

Dynamic mechanical analysis (DMA) was performed on DMA Q800 (New Castle, DE) with a tension mode. Samples with the dimensions of 40.0 × 8.0 × 0.4 mm³ were tested from 0 to 260 °C at a heating rate of 3 °C/min and a frequency of 1 Hz.

Differential scanning analysis (DSC) measurements were carried out on DSC Q2000 (TA Instruments). The samples were heated at a rate of 10 °C/min from 0 to 200 °C under a nitrogen gas atmosphere. The degree of curing reaction can be represented by the conversion rate of curing temperature (eq S2), and the data can be given directly by a DSC instrument. Thermogravimetric analyses were performed with a TGA-1 (METTLER, Switzerland) analyzer to investigate the thermal degradation of the cured D-N blends from 45 to 800 °C at a heating rate of 10 °C/min in a nitrogen atmosphere.

Fourier transform infrared (FTIR) spectroscopy was performed on a Nicolet iS10 spectrometer (Thermo Corporation). ¹H NMR spectra of DHC and DHC-N were recorded using a Bruker 600 MHz spectrometer at room temperature. Deuterated chloroform (CDCl₃) was used as the solvent.

The tests of tensile strength and elongation at break were conducted using a WDW-50E machine in accordance with ASTM-D-3039. Specimens of dimensions 50.0 × 10.0 × 0.1–0.5 mm³ with a crosshead speed of 1 mm/min and a gauge

length of 25 mm were used to carry out the test. Impact strength was determined using the charpy impact tester (model XJJ-50) in accordance with ASTM D-256 for specimens with dimensions of 50.0 × 10.0 × 5.0 mm³.

■ ASSOCIATED CONTENT

📄 Supporting Information

The Supporting Information is available free of charge on the ACS Publications website at DOI: 10.1021/acsomega.9b02282.

Ways to calculate the conversion rate of curing temperature; reaction mechanism of epoxy resin DGEBA/dicyandiamide system (PDF)

■ AUTHOR INFORMATION

Corresponding Author

*E-mail: congli2016@163.com. Tel/Fax: 0086-531-89631681.

ORCID

Cong Li: 0000-0002-1511-6255

Notes

The authors declare no competing financial interest.

■ ACKNOWLEDGMENTS

We thank Natural Science Foundation of Shandong Province, China (Grant No. ZR2019MEM002) and Young Doctoral Cooperation Funds of Qilu University of Technology (Shandong Academy of Sciences), China (Grant Nos. 2018BSHZ0028 and 2018BSHZ0020) for financial support.

■ REFERENCES

- (1) Marriam, I.; Xu, F. J.; Tebyetekerwa, M.; Gao, Y.; Liu, W.; Liu, X. H.; Qiu, Y. P. Synergistic effect of CNT films impregnated with CNT modified epoxy solution towards boosted interfacial bonding and functional properties of the composites. *Composites, Part A* **2018**, *110*, 1–10.
- (2) Nissilä, T.; Hietala, M.; Oksman, K. A method for preparing epoxy-cellulose nanofiber composites with an oriented structure. *Composites, Part A* **2019**, *125*, No. 105515.
- (3) Sugiman, S.; Putra, I. K. P.; Setyawan, P. D. Effects of the media and ageing condition on the tensile properties and fracture toughness of epoxy resin. *Polym. Degrad. Stab.* **2016**, *134*, 311–321.
- (4) Tian, N.; Ning, R.; Kong, J. Self-toughening of epoxy resin through controlling topology of cross-linked networks. *Polymer* **2016**, *99*, 376–385.
- (5) Lobanov, M. V.; Gulyaev, A. I.; Babin, A. N. Improvement of the impact and crack resistance of epoxy thermosets and thermoset-based composites with the use of thermoplastics as modifiers. *Polym. Sci., Ser. B* **2016**, *58*, 1–12.
- (6) Sprenger, S. Epoxy resin composites with surface-modified silicon dioxide nanoparticles: A review. *J. Appl. Polym. Sci.* **2013**, *130*, 1421–1428.
- (7) Cai, X.; Han, T.; Li, C.; Yang, Z.; Qiao, C. Research progress on toughening modification of epoxy resin. *J. Qilu Univ. Technol.* **2019**, *33*, 29–34.
- (8) Hodgkin, J. H.; Simon, G. P.; Varley, R. J. Thermoplastic toughening of epoxy resins: a critical review. *Polym. Adv. Technol.* **1998**, *9*, 3–10.
- (9) Bakar, M.; Bialkowska, A.; Kuřitka, I.; Hanulíková, B.; Masář, M. Synergistic effects of thermoplastic and nanoclay on the performance properties and morphology of epoxy resin. *Polym. Compos.* **2018**, *39*, 2540–2551.
- (10) Domun, N.; Hadavinia, H.; Zhang, T.; Sainsbury, T.; Liaghat, G. H.; Vahid, S. Improving the fracture toughness and the strength of epoxy using nanomaterials—a review of the current status. *Nanoscale* **2015**, *7*, 10294–10329.

- (11) Eksik, O.; Maiorana, A.; Spinella, S.; Krishnamurthy, A.; Weiss, S.; Gross, R. A.; Koratkar, N. Nanocomposites of a Cashew Nut Shell Derived Epoxy Resin and Graphene Platelets: From Flexible to Tough. *ACS Sustainable Chem. Eng.* **2016**, *4*, 1715–1721.

- (12) Tahami, H. V.; Ebrahimi, M.; Yahyaei, H.; Mafi, E. R.; Bagheri, R. Investigation of the Role of Rubber Particle Cavitation Resistance on the Toughening Mechanisms of Epoxy Resins. *J. Compos. Biodegrad. Polym.* **2016**, *4*, 16–25.

- (13) Hsieh, T. H.; Kinloch, A. J.; Taylor, A. C.; Kinloch, I. A. The effect of carbon nanotubes on the fracture toughness and fatigue performance of a thermosetting epoxy polymer. *J. Mater. Sci.* **2011**, *46*, 7525–7535.

- (14) Ren, X.; Tu, Z.; Wang, J.; Jiang, T.; Yang, Y.; Shi, D.; Mai, Y. W.; Shi, H.; Luan, S.; Hu, G. H. Critical rubber layer thickness of core-shell particles with a rigid core and a soft shell for toughening of epoxy resins without loss of elastic modulus and strength. *Compos. Sci. Technol.* **2017**, *153*, 253–260.

- (15) Lee, S. E.; Jeong, E.; Lee, M. Y.; Lee, M. K.; Lee, Y. S. Improvement of the mechanical and thermal properties of polyethersulfone-modified epoxy composites. *J. Ind. Eng. Chem.* **2016**, *33*, 73–79.

- (16) Rafique, I.; Kausar, A.; Anwar, Z.; Muhammad, B. Exploration of Epoxy Resins, Hardening Systems, and Epoxy/Carbon Nanotube Composite Designed for High Performance Materials: A Review. *Polym.-Plast. Technol. Eng.* **2016**, *55*, 312–333.

- (17) Shin, H.; Kim, B.; Han, J. G.; Lee, M. Y.; Park, J. K.; Cho, M. Fracture toughness enhancement of thermoplastic/epoxy blends by the plastic yield of toughening agents: A multiscale analysis. *Compos. Sci. Technol.* **2017**, *145*, 173–180.

- (18) Kumar, S.; Krishnan, S.; Samal, S. K.; Mohanty, S.; Nayak, S. K. Toughening of Petroleum Based (DGEBA) Epoxy Resins with Various Renewable Resources Based Flexible Chains for High Performance Applications: A Review. *Ind. Eng. Chem. Res.* **2018**, *57*, 2711–2726.

- (19) Liu, W.; Zhou, R.; Goh, H. L.; Huang, S.; Lu, X. From waste to functional additive: toughening epoxy resin with lignin. *ACS Appl. Mater. Interfaces* **2014**, *6*, 5810–5817.

- (20) Mashouf, R. G.; Mohanty, A. K.; Misra, M. Green Approaches To Engineer Tough Biobased Epoxies: A Review. *ACS Sustainable Chem. Eng.* **2017**, *5*, 9528–9541.

- (21) Li, Y.; Yang, L.; Zhang, H.; Tang, Z. Synthesis and curing performance of a novel bio-based epoxy monomer from soybean oil. *Eur. J. Lipid Sci. Technol.* **2017**, *119*, No. 1600429.

- (22) Sahoo, S. K.; Mohanty, S.; Nayak, S. K. Toughened bio-based epoxy blend network modified with transesterified epoxidized soybean oil: synthesis and characterization. *RSC Adv.* **2015**, *5*, 13674–13691.

- (23) Tan, S. G.; Chow, W. S. Biobased Epoxidized Vegetable Oils and Its Greener Epoxy Blends: A Review. *Polym.-Plast. Technol. Eng.* **2010**, *49*, 1581–1590.

- (24) Sahoo, S. K.; Mohanty, S.; Nayak, S. K. Mechanical, Thermal, and Interfacial Characterization of Randomly Oriented Short Sisal Fibers Reinforced Epoxy Composite Modified with Epoxidized Soybean Oil. *J. Nat. Fibers* **2017**, *14*, 357–367.

- (25) Fei, X.; Wei, W.; Zhao, F.; Zhu, Y.; Luo, J.; Chen, M.; Liu, X. Efficient Toughening of Epoxy-Anhydride Thermosets with a Biobased Tannic Acid Derivative. *ACS Sustainable Chem. Eng.* **2017**, *5*, 596–603.

- (26) Wang, X.; Zhou, S.; Guo, W. W.; Wang, P. L.; Xing, W.; Song, L.; Hu, Y. Renewable Cardanol-Based Phosphate as a Flame Retardant Toughening Agent for Epoxy Resins. *ACS Sustainable Chem. Eng.* **2017**, *5*, 3409–3416.

- (27) Lipatov, Y. S.; Alekseeva, T. T. Phase-Separated Interpenetrating Polymer Networks. *Adv. Polym. Sci.* **2007**, *208*, 1–227.

- (28) Roudsari, G. M.; Mohanty, A. K.; Misra, M. Exploring the Effect of Poly(propylene carbonate) Polyol in a Biobased Epoxy Interpenetrating Network. *ACS Omega* **2017**, *2*, 611–617.

- (29) Li, C.; Sung, J.; Sun, X. S. Network from Dihydrocoumarin via Solvent-Free Metal-Mediated Pathway: A Potential Structure for

Substantial Toughness Improvement of Epoxidized Plant Oil Materials. *ACS Sustainable Chem. Eng.* **2016**, *4*, 1231–1239.

(30) Van Zee, N. J.; Coates, G. W. Alternating copolymerization of dihydrocoumarin and epoxides catalyzed by chromium salen complexes: a new route to functional polyesters. *Chem. Commun.* **2014**, *50*, 6322–6325.

(31) Li, C.; Cao, D.; Guo, W.; Wu, C. The Investigation of Miscibility in Blends of ENR/AO-80 by DMA and FT-IR. *J. Macromol. Sci., Part B: Phys.* **2007**, *47*, 87–97.

(32) Mollón, V.; Bonhomme, J.; Viña, J.; Argüelles, A.; Fernández, C. A. Influence of the principal tensile stresses on delamination fracture mechanisms and their associated morphology for different loading modes in carbon/epoxy composite. *Composites, Part B* **2012**, *43*, 1676–1680.

(33) Purslow, D. Matrix fractography of fibre-reinforced epoxy composites. *Composites* **1986**, *17*, 289–303.